Available online at www.sciencedirect.com
ScienceDirect
Catalysis Today 117 (2006) 337–342
CATALYSIS TODAY
www.elsevier.com/locate/cattod

Chromium-incorporated TUD-1 as a new visible light-sensitive photo-catalyst for selective oxidation of propane

M.S. Hamdy [a], O. Berg [b], J.C. Jansen [c], Th. Maschmeyer [d], A. Arafat [e], J.A. Moulijn [a], G. Mul [a,*]

[a] *R&CE, DelftChemTech., TU Delft, Julianalaan 136, 2628 BL, Delft, The Netherlands*
[b] *Leiden Institute of Chemistry, Leiden University, Einsteinweg 55, P.O. Box 9502, 2300 RA Leiden, The Netherlands*
[c] *The Pore, DelftChemTech., TU Delft, Julianalaan 136, 2628 BL, Delft, The Netherlands*
[d] *Laboratory of Applied Catalysis for Sustainability, School of Chemistry, The University of Sydney, Sydney, NSW 2006, Australia*
[e] *Laboratory of Organic Chemistry, Wageningen University, Drijenplein 8, 6703 HB, Wageningen*

Available online 7 July 2006

Abstract

Chromium was incorporated in the framework of TUD-1 mesoporous silica by a one-pot synthesis procedure, using triethanolamine as a bi-functional template. The Cr-TUD-1 catalyst was characterized by means of X-ray diffraction, high-resolution transmission electron microscopy, UV–vis and Raman spectroscopy, as well as elemental analysis and N_2 sorption measurements. The results indicate that chromium is incorporated as tetrahedrally co-ordinated Cr^{6+} in the framework of TUD-1. When tested as a catalyst for the photo-oxidation of propane, Cr-TUD-1 showed high activity and high selectivity towards acetone under visible light irradiation ($\lambda = 435$ nm).
© 2006 Published by Elsevier B.V.

Keywords: Mesoporous; Chromium; Cr-TUD-1; Photo-catalysis; Propane; Acetone

1. Introduction

Transformation of light alkanes to value-added products such as alkenes and oxygenates is one of the main challenges of the refining and petrochemical industries [1]. Among others, Cr-based catalysts have received extensive attention in the literature for the direct dehydrogenation of propane, which has been studied over different chromium catalysts (mainly Al_2O_3 and ZrO_2 based) [2, and references therein]. Dehydrogenation of alkanes to alkenes can also be accomplished under oxidative conditions (oxidative dehydrogenation), the advantage of this method being that it is operative at much lower temperatures than direct dehydrogenation [3,4]. However, the main limitation of this process is that it requires a selective catalyst in order to avoid complete oxidation to CO and CO_2. Busca introduced $MgCr_2O_4$ as an active catalyst for oxidation of light hydrocarbons, but generally selective oxidation products were only observed at relatively low conversion [5–7]. The reaction mechanism was investigated by means of infrared spectroscopy, showing that propane oxidation involves an intermediate activated at C2 (2-propoxy species were observed). In general it can be concluded that Cr-catalysts are inherently not very selective in oxidation processes, i.e. in oxidative dehydrogenation or the direct synthesis of oxygenates. Improvement of the oxidative selectivity of Cr-catalysts is therefore required, either by means of catalyst modification or – taking advantage of the rich spectroscopic structure of Cr ions – by low-temperature activation using light.

Recently Cr-based photo-catalysts, which intrinsically have a higher sensitivity to visible light than TiO_2 [8–10], have been reported in the literature, either in the presence or absence of a TiO_2 co-catalyst. One class of Cr-catalysts is $MCrO_4$ (M = Ba, Sr), the d^0 electrons of which were the first to show a catalyic response to visible light [11]. Smirniotis and co-workers studied chromium loaded on different TiO_2 phases and its various catalytic properties [12–14]. An important reported application [15] was the photo-catalytic degradation of aqueous organic molecules (e.g. formic acid, 2,4,6-trichlorophenol, and 4-chlorophenol) by visible light irradiation. Results showed that TiO_2/Cr–Ti–MCM-41 was photo-catalytically more active

* Corresponding author. Tel.: +31 15 2786197; fax: +31 15 2784005.
E-mail address: G.Mul@tnw.tudelft.nl (G. Mul).

0920-5861/$ – see front matter © 2006 Published by Elsevier B.V.
doi:10.1016/j.cattod.2006.05.058

than Degussa P-25 at visible wavelengths; however, it was less active under UV irradiation. Anpo and co-workers reported the photo-catalytic activity of chromium-incorporated HMS mesoporous material [16–18] and chromium-incorporated ZSM-5 zeolites [19] for selective oxidation. Results clearly showed the photo-catalytic efficacy of Cr^{6+} in the framework of both silica and silica–alumina supports. With 2% by weight of Cr loaded in HMS, excited at wavelengths $\lambda > 450$ nm, propane was converted to acetone with a selectivity of almost 20%, with 40% converted to CO/CO_2, and the rest to various hydrocarbons.

In this paper, chromium-TUD-1 [20] is introduced as a new visible light-sensitive photo-catalyst for propane photo-oxidation. In the present work narrow-band excitation centred around 435 nm was used to activate the catalyst, while product composition was determined on the surface of the catalysts, rather than in the gas phase, by applying *operando* infrared spectroscopy.

2. Experimental

2.1. Cr-TUD-1 synthesis

Cr-TUD-1 was synthesized by aging, drying, and calcination of a homogeneous synthesis mixture. The latter consists of a solution of chromium nitrate nonahydrate ($Cr(NO_3)_3{\cdot}9H_2O$), a silicon alkoxide source (tetraethyl orthosilicate (TEOS)), and triethanolamine (TEA). An aqueous chromium salt solution (0.38 g of chromium nitrate + 2 mL of H_2O) was added dropwise into TEOS (19.91 g, +98%, ACROS). While stirring, a mixture of 14.4 g of TEA (97%, ACROS) + 3.6 mL of H_2O was added dropwise. Finally, 19.7 g of tetraethyl ammonium hydroxide (TEAOH, 35%, Aldrich) was added, again dropwise. After stirring for 2 h, a clear and pale green solution was obtained, with a molar ratio composition of SiO_2:0.01Cr_2O_3:0.5-TEAOH:11H_2O. The mixture was aged at room temperature for 24 h, dried at 100 °C for 24 h, hydrothermally treated in a stainless steel Teflon-lined autoclave, and then calcined at 600 °C for 10 h using a heating ramp rate of 1 °C/min in air. The final product was a pale yellow powder with a Si/Cr ratio of 130 (as obtained from elemental analysis), which is equivalent to 1 wt.% Cr.

2.2. Characterization techniques

The X-ray powder diffraction (XRD) pattern was recorded using Cu Kα radiation on a Philips PW 1840 diffractometer equipped with a graphite monochromator. The sample was scanned over a range of 0.1–80° 2θ with steps of 0.02°. High-resolution transmission electron microscopy (HR-TEM) was carried out on a Philips CM30UT electron microscope with a field emission gun, operated at 300 kV, as the source of electrons. The diffuse reflectance UV–vis spectrum was recorded using a CaryWin 300 spectrometer with $BaSO_4$ as reference. The sample was ground, heated overnight to 180 °C, and then scanned from 190 to 800 nm.

Raman spectra were recorded on a Jobin-Yvon Labram spectrometer, equipped with a 325 nm UV laser and the necessary notch filters to remove the Raleigh scattering from the Raman signal. The high sensitivity of the equipment typically allows the recording of the Raman spectra in tens of seconds to a few minutes of laser exposure.

Nitrogen sorption isotherms were recorded on a Quantachrome Autosorb-6B at 77 K. Mesoporosity was calculated from the adsorption branch using the BJH model. Elemental analysis was carried out by instrumental neutron activation analysis (INAA) on the ''Hoger Onderwijs Reactor'' nuclear reactor (thermal power of 2 MW, maximum neutron flux 2×10^{17} m^{-2} s^{-1}).

2.3. Photo-catalytic reaction

A 500 W capillary Hg arc lamp (Philips SP500) in conjunction with a grating monochromator was used as a visible light source. The bandpass of this illuminator was approximately 15 nm, and its output was measured with a thermopile power meter. Cr-TUD-1 wafers were formed on an automatic press (SPECTA) by applying 3 t/cm^2. The samples were edge-mounted on a copper sample holder in contact with a heating coil and type K thermocouples. The sample holder was placed in a stainless steel high vacuum chamber; CaF_2 windows allowed for simultaneous visible light irradiation and FT-IR spectroscopy.

All samples were activated prior to use by ramping to 300 °C at 10 deg/min, and dwelling at this temperature for 15 min under high vacuum (10^{-6} mbar range). After cooling, the cell was loaded with 2.8 mbar of propane gas and 400 mbar of molecular oxygen (1propane: 140oxygen). Because of the relatively large reactor volume, the reactions took place under a large excess of reagent gas (compared to the adsorption capacity of the sample wafer) and thus at effectively constant composition. The photo-catalytic reactions were monitored in situ by a Bio-Rad FT-IR spectrometer (175C). Light (15 mW cm^{-2}) at a wavelength of 435 nm was used to excite the samples. The spectroscopic assignments and photometric calculations have been described in detail elsewhere [21]; after deconvolution of the spectra, product concentrations were obtained using an integrated cross-section of 3.24×10^{-17} cm/molecule for the carbonyl stretch of acetone (obtained by systematic dosing) and 4.7×10^{-17} cm/molecule for carboxylates [21B]. The molar quantities of products are reported as ''column density'' — moles per unit area normal to the infrared beam. In our experimental geometry this is equivalent to moles per unit *external* area of the sample wafer. The internal area available for adsorption is orders of magnitude greater [21].

3. Results and discussion

3.1. Cr-TUD-1 as a mesoporous material

Fig. 1 shows the powder X-ray diffraction (XRD) pattern of the Cr-TUD-1 sample. The pattern shows a single intense peak at 1.5° 2θ, indicating that Cr-TUD-1 is a meso-structured material. Moreover, there is no detectable Cr_2O_3 phase or any other crystalline chromia compound. The HR-TEM images

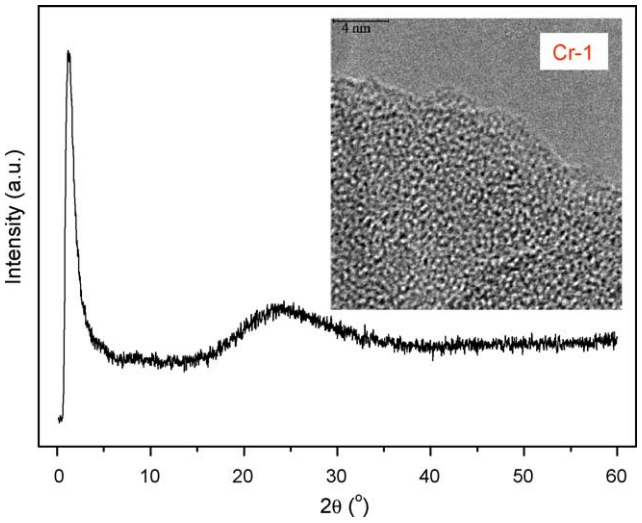

Fig. 1. X-ray diffraction pattern of calcined Cr-TUD-1. (Inset) A high-resolution electron micrograph of the same material.

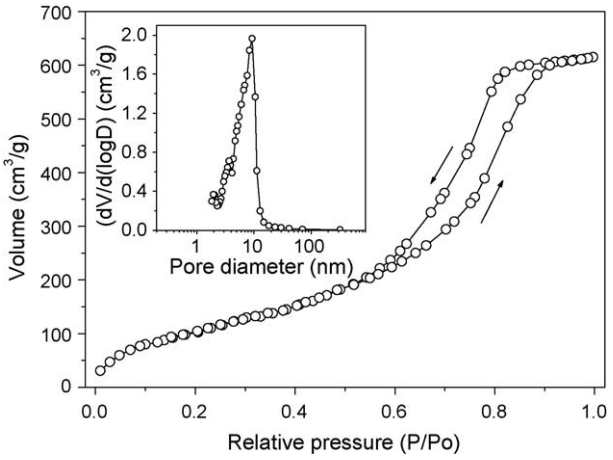

Fig. 3. Nitrogen sorption isotherm for Cr-TUD-1 at 77 K. (Inset) The corresponding mesopore size distribution.

(inset of Fig. 1) show only the sponge-like 3D structure characteristic of the TUD-1 mesoporous material (consistent with XRD). This is a strong indication for the complete isolation of Cr-atoms inside the framework. The UV–vis spectrum of the calcined Cr-TUD-1 sample is shown in Fig. 2A. Two bands around 265 and 360 nm dominate the spectrum, while a shoulder around 440 nm is also clearly present. The UV–Raman spectrum of the Cr-TUD-1 sample is presented in Fig. 2B. A single intense Raman peak around 979 cm^{-1} is charateristic of the Cr-TUD-1 sample. The UV absorption bands centered at 265 and 360 nm are usually assigned to a charge-transfer absorption, inducing an electron transition from O^{2-} to Cr^{6+} of tetrahedrally co-ordinated isolated Cr^{6+}, symbolically $(Cr^{5+}–O^{-1})^{*} \leftarrow (O^{2-}=Cr^{6+})$ [22,23]. This absorption thus confirms the presence of isolated Cr^{VI} atoms inside the silica matrix. This is in good agreement with the observed Raman frequency of 979 cm^{-1}, which is assigned to highly dispersed isolated monochromate species [22]. The 440 nm absorption in the UV–vis spectrum is more difficult to explain. It has been proposed in the literature that this absorption is related to Cr–O–Cr linkages in polymeric chromia species, while it has also been demonstrated that distorted isolated sites contribute to the absorption. In view of the absence of Raman bands that are typically assigned to di-, or polychromate species, distorted isolated chromate species are proposed to dominate the observed absorption at around 440 nm. As a final note, no peaks were detected at wavelengths greater than 600 nm, where octahedral Cr^{III} would be expected (again consistent with the XRD result).

The N_2 adsorption–desorption isotherm for the Cr-TUD-1 sample is shown in Fig. 3. This typical ''type IV'' isotherm is indicative for a meso-structured material. The characteristics of the Cr-TUD-1 sample calculated from the adsorption branch of the N_2 isotherm, using the Barrett–Joyner–Halenda formula, are as follows: the surface area of the sample is 565 m^2/g, the pore volume is 1.54 cm^3/g, and the pore size distribution curve (inset of Fig. 3) peaks at 8.2 nm.

3.2. Photo-catalytic performance

By testing the component materials separately it can be shown that the Cr-TUD-1 composite is responsible for the photo-activity observed. A comparison of the spectra obtained after 100 min of reaction for siliceous TUD-1, pure Cr_2O_3, and Cr-TUD-1 is given in Fig. 4. For TUD-1 and Cr_2O_3 only a minor signal due to adsorbed acetone (C=O stretch at 1685 cm^{-1}) is observed. For Cr-TUD-1 this signal is more intense by a factor of 10. In this case additional bands due to

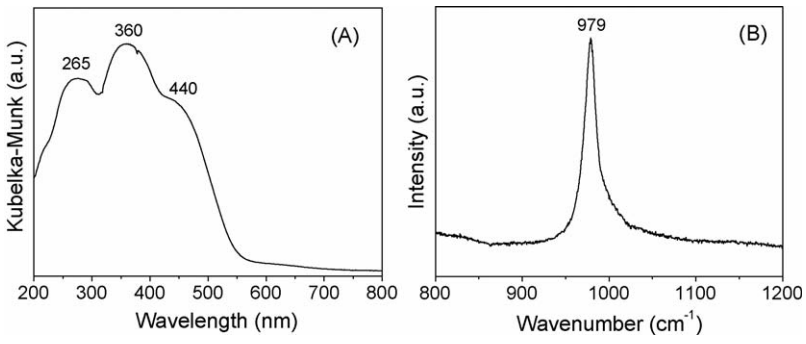

Fig. 2. (A) Diffuse–reflectance UV–vis spectrum of calcined Cr-TUD-1 at ambient conditions. (B) UV–Raman spectrum of calcined Cr-TUD-1.

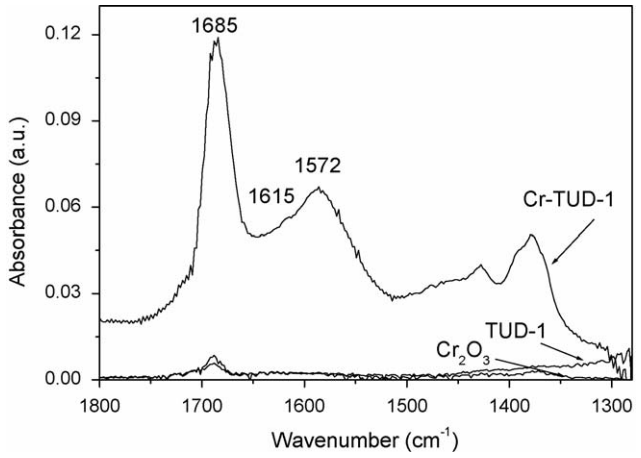

Fig. 4. The infrared spectra of adsorbed products on Cr-TUD-1, TUD-1, and Cr_2O_3 surfaces, recorded after 100 min of propane photo-oxidation.

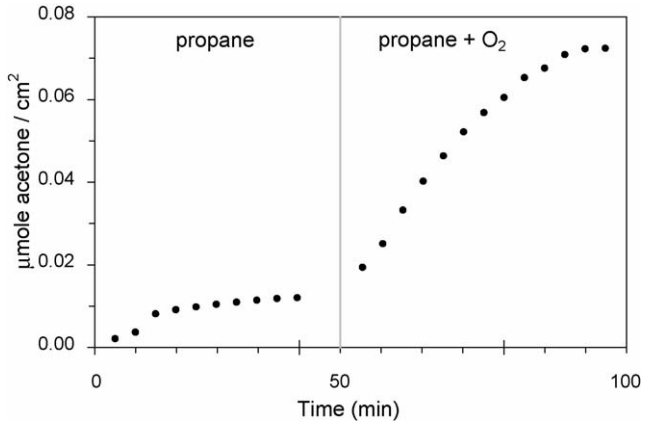

Fig. 5. Molar acetone production as a function of irradiation time without (left) and with (right) the presence of oxygen gas.

carboxylate stretches (1572 cm^{-1}) and C–H bending modes (1435 cm^{-1}) are also detected. It is concluded that the presence of Cr^{VI} species greatly increases the photo-catalytic yield under 435 nm excitation. These spectra also show that complete oxidation (combustion) is not the dominant reaction path. Although not strongly adsorbed, CO_2 is easily detectable at low coverage because of its large infrared cross-section; and water, which is strongly adsorbed, is indicated by its bending mode at 1635 cm^{-1}. CO_2 does not appear in the (extended) product spectra of Cr-TUD-1, and the coverage of water deduced by deconvoluting the product spectra is not disproportionate.

It is interesting that some of the oxygen native to the Cr-TUD-1 solid can be consumed under photochemical reaction conditions. In Fig. 5 the column density of adsorbed acetone is plotted as a function of irradiation time. To the left of the grey vertical line, the only gas-phase reagent is propane. To the right, the same partial pressure of propane is mixed with molecular oxygen. Acetone is certainly generated during the first period, but the rate levels off after the first 20 min of the trial. With the addition of oxygen gas, not only does the absolute reaction rate exceed its initial value, but this falls off with a larger time constant. Since a significant fraction of this acetone will desorb under high vacuum conditions, this reaction falls under the broad definition of photo-catalysis [23b]. The data in Fig. 5 can now be used to estimate its efficiency. The initial rate of acetone formation in the presence of oxygen gas is 1.4×10^{13} molecules/(cm^2 s). The excitation intensity corresponds to 3.3×10^{16} photons/s, of which none are transmitted by the sample wafer. The yield of acetone is therefore 4.2×10^{-4} molecules per photon. This may be regarded as a lower limit for the intrinsic photochemical yield, as light lost by backscattering from the sample wafer has been neglected.

The effects of illumination and temperature are evident in Fig. 6. Propane consumption (acetone + carboxylate production) is plotted as a function of time, during which illumination was switched on and off, at 25 °C (Fig. 6A) and 55 °C (Fig. 6B). The illumination was chosen so as to give a convenient acetone signal level: 100 min at 25 °C, and only 10 min at 55 °C. The initial photochemical reaction rate is clearly greater at the higher temperature. In both cases the dark reaction rate is negligible in comparison to the photochemical rate. Although slow, the dark reaction that follows a period of photochemistry has a different stoichiometry. The inset to Fig. 6A shows a difference spectrum of the dark period only (280-min spectrum–100-min spectrum). A small amount of carboxylates grow in at the expense of acetone, which has either reacted or desorbed. On these grounds we conclude that the absorption of light is responsible for the accelerated production of both

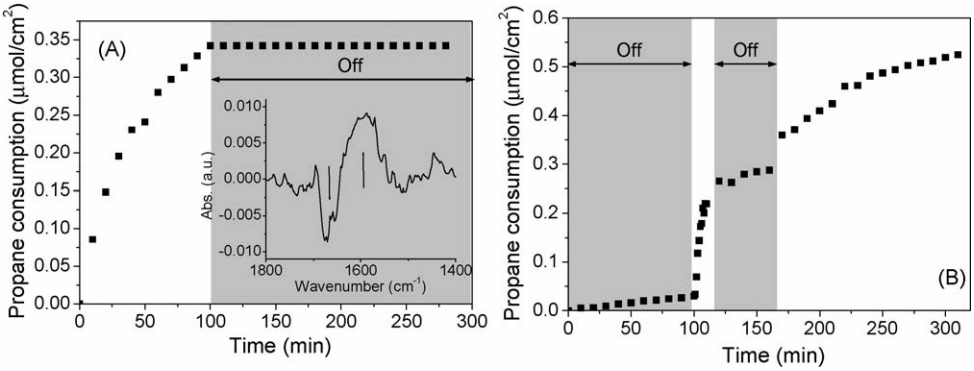

Fig. 6. Molar propane consumption (acetone + carboxylates/2) as a function of time at 25 °C (Fig. 5A) and 55 °C (Fig. 5B), with and without irradiation. Shaded areas indicate periods without irradiation. Inset of (A) difference spectrum of the dark period indicated (after–before), illustrating the slow interconversion of acetone to carboxylates.

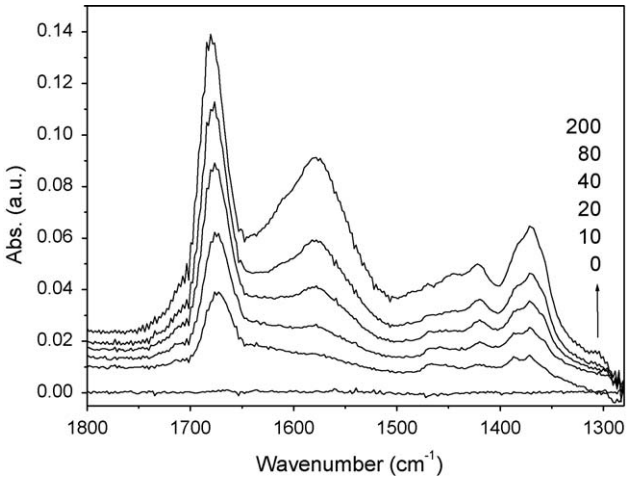

Fig. 7. The development of infrared absorbance spectra during photo-catalytic oxidation of propane over Cr-TUD-1 with 435 nm illumination.

acetone and carboxylates, and that its effect is not simply to raise the local temperature.

Fig. 7 shows the evolution of the product spectrum as a function of illumination time. Acetone is prominent in the early spectra (1685 cm^{-1}), but at later times the relative intensity of the carboxylate band increases (1572 cm^{-1}). The absolute column density of acetone and carboxylates can be quantified by deconvoluting these peaks, integrating them, and applying the Lambert–Beer law; the results of such an analysis are plotted in Fig. 8A. It is striking that the rate of carboxylate production is constant. Meanwhile the acetone production rate – initially greater than the carboxylate production rate – decreases monotonically and falls off below the rate of carboxylate production. These data can be recast in terms of the overall propane consumption, and selectivity toward acetone, as plotted in Fig. 8B.

The species involved in propane activation over the Cr-TUD-1 catalyst are shown schematically in Fig. 9. Although in the literature there is still debate concerning the exact structure of isolated Cr-species on silica surfaces (mono-, or di-oxo), recent data indicate that largely di-oxo species are exposed [24]. When the Cr-TUD-1 sample is illuminated a charge transfer from O^{2-} to Cr^{6+} yields $(Cr^{5+}–O^{-1})^{*}$, and the reactive oxygen atom initiates chemistry with adsorbed molecules. It is likely that a proton is abstracted from propane, forming a

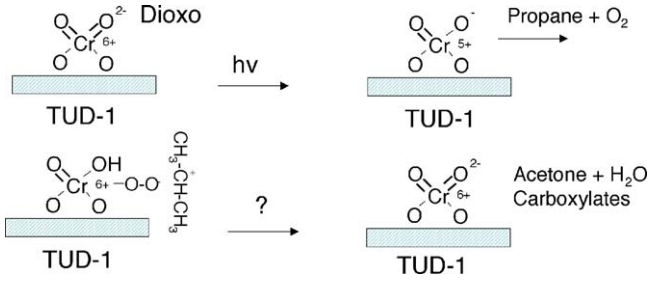

Fig. 9. Schematic illustration of known and suspected steps in the photo-catalyzed oxidation of propane.

hydroxyl group and a propane radical cation. The subsequent formation of acetone, in Fig. 9 for the presence of oxygen tentatively proposed to proceed *via* a peroxo-intermediate, suggests that propane is activated at C2, which agrees with the lower dissociation energy of C–H at secondary carbon atoms compared with primary ones [25,26]. Compounds produced as a result of C1 oxidation, such as the aldehyde or acid, were not detected (consistent with Ref. [27]).

Since these reaction steps are speculative, they may be contrasted to propane oxidation as it occurs in cation-exchanged zeolites. In the latter case the presumed first step is direct electron transfer from propane to oxygen; these radicals react directly to form the C2 hydroperoxide. In a zeolite matrix this intermediate can be identified directly by its infrared spectrum, and indirectly by its slow decomposition (dark reaction) following a period of photochemical activation [28,29]. Neither is observed in Cr-TUD-1. The absence of an acetone-forming dark reaction argues against the participation of a hydroperoxide intermediate (Fig. 6), while the formation of acetone in the absence of molecular oxygen (Fig. 5) suggests that oxygen atoms can be abstracted from the matrix. These ideas can and will be tested by means of isotopic labelling.

Although the reaction on Cr-TUD-1 is less selective than on zeolites, the lower binding energy of acetone and water allows them to be removed at lower temperature. The carboxylates were not desorbed under these conditions, and could only be decomposed by treatment with O_2 at 500 °C. The photochemical activity of a used sample did recover after this oxidative treatment, albeit incompletely. The initial reaction rate after oxidative treatment was approximately 50% lower than in a fresh sample, even though carboxylates and carbonates could no

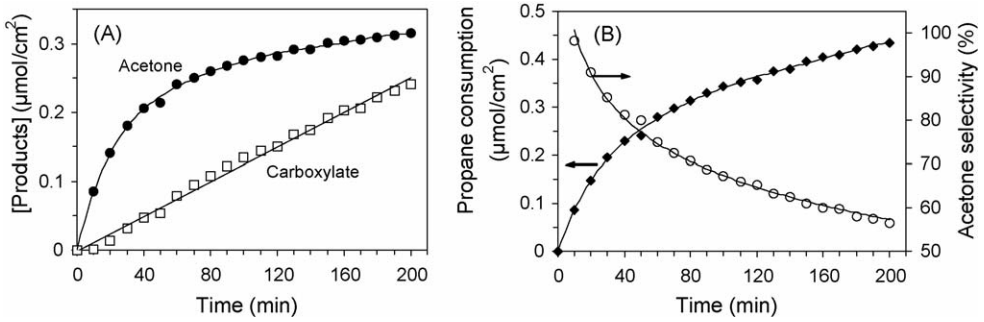

Fig. 8. (A) The appearance of adsorbed photochemical products during 200 min of irradiation. (B) Propane conversion and acetone selectivity plotted during the same period.

longer be detected at the surface. The reason for the decreasing performance requires further investigation.

4. Conclusion

A new catalytic material, Cr-TUD-1 with a Si/Cr ratio of 130, was prepared in a one-pot synthesis procedure. Chromium is present in this material primarily as isolated tetrahedral (di-oxo) Cr^{6+} species, and those on the silica surface can selectively photo-catalyze the dehyrogenation of propane under blue light.

Acknowledgements

Prof. I.E. Wachs and Dr. S. Choi are gratefully acknowledged for the Raman measurements. Hamdy thanks Helwan University-Egyptian Government for a personal fellowship. The work was financially support by STW, the Netherlands.

References

[1] K.K. Kearby, in: P.H. Emmet (Ed.), Catalysis, vol. 3, Reinhold, New York, 1955, p. 453.
[2] T.A. Nijhuis, S.J. Tinnemans, T. Visser, B.M. Weckhuysen, Chem. Eng. Sci. 59 (2004) 5487.
[3] H.H. Kung, Adv. Catal. 40 (1994) 1.
[4] S. Albonetti, F. Cavani, F. Trifiro, Catal. Rev.-Sci. Eng. 38 (1996) 413.
[5] E. Finocchio, G. Busca, V. Lorenzelli, J. Chem. Soc. Faraday Trans. 90 (1994) 3347.
[6] E. Finocchio, G. Ramis, G. Busca, V. Lorenzelli, R.J. Willey, Catal. Today 28 (1996) 381.
[7] G. Busca, M. Daturi, E. Finocchio, V. Lorenzelli, G. Ramis, R.J. Willey, Catal. Today 33 (1997) 239.
[8] A. Fujishima, K. Honda, Nature 238 (1972) 37.
[9] R. Asahi, T. Morikawa, T. Ohwaki, K. Aoki, Y. Taga, Science 293 (2001) 269.
[10] Z. Zou, J. Ye, K. Sayama, H. Arakawa, Nature (Lond.) 414 (2001) 625.
[11] A. Kudo, K. Ueda, H. Kato, I. Mikami, Catal. Lett. 53 (1998) 229.
[12] P.G. Smirniotis, D.A. Pena, B.S. Uphade, Angew. Chem. Int. Ed. 40 (2001) 2479.
[13] D.A. Pena, B.S. Uphade, E.P. Reddy, P.G. Smirniotis, J. Phys. Chem. B 108 (2004) 9927.
[14] D.A. Pena, B.S. Uphade, P.G. Smirniotis, J. Catal. 221 (2004) 421.
[15] L. Davydov, E. Reddy, P. France, P.G. Smirniotis, J. Catal. 203 (2001) 157.
[16] H. Yamashita, M. Ariyuki, S. Higashimoto, S.G. Zhang, J.S. Chang, S.E. park, J.M. Lee, Y. Matsumura, M. Anpo, J. Synchrotron Rad. 6 (1999) 543.
[17] H. Yamashita, K. Yoshizawa, M. Ariyuki, S. Higashimoto, M. Che, M. Anpo, Chem. Commun. (2001) 435.
[18] H. Yamashita, M. Ariyuki, K. Yoshizawa, K. Kida, S. Ohshiro, M. Anpo, Res. Chem. Intermed. 30 (2004) 235.
[19] H. Yamashita, S. Ohshiro, K. Kida, K. Yoshizawa, M. Anpo, Res. Chem. Intermed. 29 (2003) 881.
[20] Z. Shan, M.S. Hamdy, J.C. Jansen, C. Yeh, P. Angevine, Th. Maschmeyer, U.S. Patent 6930219 (2005) and WO Patent Appl. 2004052537 (2004).
[21] (a) M.S. Hamdy, O. Berg, J.C. Jansen, Th. Maschmeyer, J.A. Moulijn, G. Mul, Chem. Eur. J., in press.
(b) V.A. Matyshak, O.V. Krylov, Kinet. Catal. 43 (2002) 422.
[22] B.M. Weckhuysen, I.E. Wachs, R.A. Schoonheydt, Chem. Rev. 96 (1996) 3327.
[23] (a) J.S. Mambrim, H.O. Pastore, C.U. Davanzo, E.J. Vichi, O. Nakamura, H. Vargas, Chem. Mater. 5 (1993) 166;
(b) V. Parmon, A.V. Emeline, N. Serpone, Int. J. Photoenergy 4 (2002) 91.
[24] I.E. Wachs, Personal communication.
[25] A. Bielanski, J. Haber, Oxygen in Catalysis, Marcel Dekker, New York, 1991.
[26] E. Finocchio, R. Willey, G. Busca, V. Lorenzelli, J. Chem. Soc.: Faraday Trans. 93 (1997) 175.
[27] Y.Y. Yao, J. Catal. 28 (1947) 139.
[28] F. Blatter, H. Sun, S. Vasenkov, H. Frei, Catal. Today 41 (1998) 297.
[29] J. Xu, B.L. Mojet, J.G. van Ommen, L. Lefferts, J. Phys. Chem. B 108 (2004) 218.